Numerical Model for the Vacuum Pyrolysis of Scrap Tires in Batch Reactors

Jin Yang, Philippe A. Tanguy, and Christian Roy
Dept. de génie chimique, Université Laval, Québec, Canada G1K 7P4

A quantitative model for scrap tire pyrolysis in a batch scale reactor developed comprises the following basic phenomena: conduction inside tire particles; conduction, convection, and radiation between the feedstock particles or between the fluids and the particles; tire pyrolysis reaction; exothermicity and endothermicity caused by tire decomposition and volatilization; and the variation of the composition and the thermal properties of tire particles. This model was used to predict the transient temperature and density distributions in the bed of particles, the volatile product evolution rate, the mass change, the energy consumption during the pyrolysis process, and the pressure history in a tire pyrolysis reactor with a load of 1 kg. The model predictions agree well with independent experimental data.

Introduction

Pyrolysis has become an attractive solution to the growing environmental problems caused by the generational and worldwide accumulation of scrap tires. This approach, which has been under development over the last twenty years, is based on the air-free thermal decomposition of tires at high temperature (450–800°C) to useful products such as carbon black, pyrolysis oils, steel and gas. Several pyrolysis processes have been proposed, such as vacuum pyrolysis (Roy et al., 1989, 1990), flash pyrolysis (Che et al. 1976), molten salt pyrolysis (Chambers et al., 1984), and a few batch processes (Araki et al., 1979; Bouvier et al., 1987; Schulman and White, 1978; William et al., 1990). The published literature deals primarily with process description, product characterization, and market surveys. Very few studies have been conducted on the fundamentals of tire pyrolysis, such as chemical kinetics and heat-transfer, and mass-transfer mechanisms. In order to foster the development of tire pyrolysis toward producing better product quality and increasing the process efficiency, a better understanding of the basic physical and chemical mechanisms underlying the process is necessary. This study is based on the fundamental research in the following areas:

- Thermal and kinetic studies by thermal analysis techniques
- Heat and mass transfer in a large single particle
- Heat and mass transfer in a packed bed of particles.

The first two research areas were investigated in previous studies (Yang et al., 1993, 1995a,b); the main results will be summarized later. The work of Wakao and Kaguei (1984) has been used for the third area cited. The objective of this work is to study the used-tire pyrolysis mechanism in a batch reactor. A mathematical model will be developed that combines a series of partial differential equations governing the kinetics of tire pyrolysis, the heat transfer inside the scrap tire particles, the conduction, convection, and radiation of heat transfer in the reactor and in the bed of particles. The model provides a quantitative description of the thermal and kinetic processes during tire pyrolysis in a batch reactor, through the prediction of the temperature distribution and tire conversion in the bed of tire particles, as well as the energy consumption, mass change, and the pressure history in the reactor. This model will be also tested using the experimental data of Labrecque (1987) for tire pyrolysis in a batch reactor.

Literature Review

Heat and mass transfer in pyrolysis batch reactors has been studied at the macroscopic and the microscopic levels. Most tire pyrolysis studies published so far only provided a macroscopic description of the process without much insight or understanding of the underlying physicochemical phenomena.

Correspondence concerning this article should be addressed to C. Roy.
Present address of P. A. Tanguy: UREPI, Ecole Polytechnique, PO Box 6079, Stn. Centre-Ville, Montréal, P. Q., Canada H3C 3A7.

For instance, Bouvier et al. (1987) investigated tire pyrolysis under nitrogen atmosphere. In their study, the bed of tire particles was simplified as a uniform system. The overall heat transfer and the chemical kinetics were studied and semitheoretical equations were developed to model the average temperature and conversion of the bed. In the experimental work of Labrecque (1987), tire pyrolysis under vacuum conditions was investigated. The mean pressure and temperature in the center of the bed were measured and the energy and mass changes were estimated as a function of temperature. Finally, the overall thermal efficiency was calculated. The total weight loss of the tire particles was found to lie between 60% and 70%. The global energy consumption was estimated to be 706 kJ/kg.

Since the scope of these results is limited to a narrow operating window, extrapolation to other experimental conditions is rather unsafe, particularly in light of the poor understanding of the mechanism of tire pyrolysis. There is clearly a need for a microscale pyrolysis investigation, from which more detailed information and quantitative data could be obtained.

At the microscopic scale, the bed temperature and concentration gradients in the axial and radial directions must be considered, due to heat transfer from the walls and from the bottom of the reactor. Each particle in the bed can be viewed as a small reactor. Heat is transferred from the adjacent tire particles by conduction and radiation, as well as from the fluid in the void space by convection. Pyrolysis develops from the surface toward the center, following the propagation of the pyrolysis temperature throughout the particle. Within the particles, the prevailing heat-transfer mechanism is conduction; some convection is also present due to the flow of the volatile materials in the porous structure. The pyrolysis of single particles has been widely investigated in previous studies mainly for wood, coal, and oil shale. Mathematical models were proposed to predict the internal mass and temperature changes under well-defined thermal conditions (Bamford et al., 1946; Becker et al., 1984; Chan et al., 1985; Havens et al., 1971; Kung, 1972; Phuoc et al., 1987; Pyle and Zaror, 1984; Stevenson et al., 1973). Recently, Yang et al. (1995b) studied the pyrolysis of single tire particles. A mathematical model was developed that included the heat transfer, mass transfer, pyrolysis kinetics, and their interactions during the pyrolysis.

A major limitation of mathematical models of pyrolysis processes is the lack of reliable thermal and kinetic data, which makes the quality of the predictions questionable. Thermal analysis techniques, including thermogravimetry (TG), differential thermal analysis (DTA), and differential scanning calorimetry (DSC) have been used to investigate the kinetic and thermal behavior of wood (Havens et al., 1971) and coal (Mahajam et al., 1976; Alula et al., 1990; Muñoz-Guillena et al., 1992) during pyrolysis. These techniques, however, only apply to tiny samples, where it was not necessary to consider the influence of heat or mass transfer in the sample.

In tire manufacturing, styrene-butadiene rubber (SBR), polybutadiene rubber (BR), natural rubber (NR), and their blends are the most frequently used elastomers. Their pyrolysis kinetics have generated considerable interest in the literature (Brazier and Nickel, 1975; Maurer, 1981; Sircar and Lamond, 1975; Yang et al., 1993). The weight-loss evolution of these elastomers under thermal decomposition conditions can be observed by the TG method. Successful first-order kinetic equation models can be derived and reliable kinetic data are obtained.

The energy change during pyrolysis is of considerable importance for the thermal and kinetic calculations. In several of the pyrolysis studies reported in the literature, this change was difficult to obtain. Quite often, it was assumed to be athermal due to the lack of reliable data (Zaror and Pyle, 1982; Pyle and Zaror, 1984). In Labrecque's work (1987), a small exothermic peak was observed in the temperature range of 300 and 400°C. Similar phenomena were found during the thermal decomposition of SBR and BR elastomers, using DSC measurements (Brazier and Schwartz, 1978). Further quantitative studies carried out by the authors (Yang and Roy, 1995a) using TG, DTA, and DSC equipment clearly revealed the presence of both endothermic and exothermic peaks. The energy-change mechanism was discussed and theoretical equations were proposed to describe the energy change as a function of temperature.

Theory

Let's consider a cylindrical vacuum pyrolysis reactor filled with tire particles randomly packed at the bottom of the reactor and forming a porous bed. When the thermal energy is transferred from the reactor wall, heating of the tire particles can be viewed as a two-stage process, depending on the particle temperature.

During the first stage, where the temperature rises from room temperature to approximately 200°C, no significant pyrolysis occurs. Chemical and physical changes associated with the pyrolysis phenomena can be ignored. The heat transferred from the reactor wall increases the bulk temperature and therefore the internal energy of the particles. The heat-transfer mechanism is quite simple and consists of radiation and conduction from the reactor to the bed, and conduction between the tire particles. No convection is considered since the pressure inside the reactor is very low. The temperature increase, however, modifies the thermal properties of the particles.

During the second stage, where the temperature rises from 200 to 500°C, the continuous input of energy toward the tire particles triggers the pyrolysis of the organic materials. First, the processing oil and the other low-boiling-point ingredients in the tires are vaporized between 200°C and 300°C. This is followed by the decomposition and evaporation of the polymers between 300°C and 500°C. The pyrolysis products consist of gas, organic vapors, and carbon black. The gas and vapors are rapidly sucked away by the vacuum pump as soon as they form, while the carbon black remains in the reactor as a solid residue product. Finally, when the bed temperature reaches 500°C or higher, all the organic materials in the bed have disappeared and a bed of carbon black particles remains in the reactor. Heat-transfer phenomena during this stage are quite complex, including radiation between particles and convection caused by the flux of volatiles at the surface of the particles. Since pyrolysis and heat transfer have a mutual influence, the phenomena are even more complex. Heat transfer promotes pyrolysis, which in turn triggers a series of chemical reactions and physical changes. These changes, especially those concerning the thermal properties

and the generation of pyrolysis heat, significantly influence the heat-transfer process. The heat of pyrolysis is mainly produced by the tire decomposition reaction and the vaporization of the pyrolysis products.

Heat-Transfer Characteristics

The study of heat transfer in packed beds finds many applications in industry, such as in coal gasification, coal-bed burning, catalysis, ion exchange, and heat regeneration (Wakao et al., 1984). Quite often heterogeneous packed beds are simplified as homogeneous systems in which average effective heat-transfer coefficients are used. The heat transfer within the fluid is usually ignored since the fluid density is very low; only the heat transfer between the particles and the fluid is considered. The following heat-transfer mechanisms occur in the general case:

1. Conduction through the solid particles
2. Conduction across the stagnant gas surrounding the points of contact between the particles
3. Conduction through the points of contact between the particles
4. Radiation between adjacent particle surfaces
5. Forced solid-gas convection.

According to the temperature level in the bed, two heat-transfer models can be worked out.

Conduction model

When the bed temperature is less than 200°C, only conduction has to be considered. Indeed, there is no gas flow (hence no convection) and the temperature is too low to account for radiation. Under such conditions, the effective thermal conductivity is primarily dependent on the thermal conductivities of the solid particle k_s, the stagnant gas k_g, and the bed properties. Several models have been published to determine the effective thermal conductivities of a packed bed of particles (Argo and Smith, 1953; Yagi et al., 1957; Beveridge and Haughey, 1971). In this study, the heat-conduction model of Deissler and Boegli (Beveridge and Haughey, 1971), which calculates the effective thermal conductivity of packed beds under low pressure was used:

$$Y = \frac{k_e}{k_g} = \epsilon_{A1} + \left(\frac{1-\alpha}{X(1-\epsilon_{A1})} + \frac{\alpha}{\epsilon_{A2} + X\epsilon_{A3}} \right)^{-1} \tag{1}$$

where

$$X = \frac{k_s}{k_g} \tag{2}$$

and

$$\alpha = f(\epsilon, n_c) \tag{3}$$

where ϵ_{A1}, ϵ_{A2}, and ϵ_{A3} are the area factors and n_c is the number of contact points. As shown in Figure 1, the unit cross-sectional area is divided into three parallel paths: ϵ_{A1} is the path of gas conduction, ϵ_{A2} the path of solid conduction, and ϵ_{A3} the path of contact conduction. The following

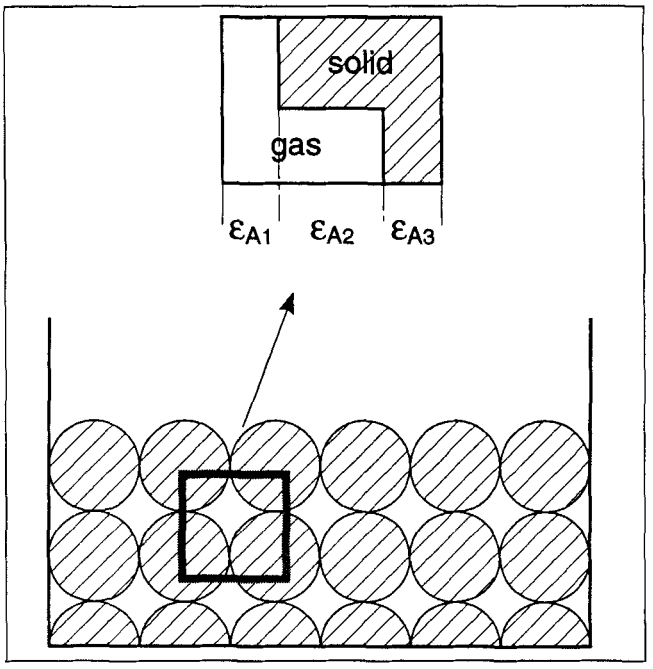

Figure 1. Unit-cell model of heat conduction in a packed bed.

relations can be derived for these various paths:

$$\epsilon_{A1} + \epsilon_{A2} + \epsilon_{A3} = 1. \tag{4}$$

The contact area, ϵ_A, depends on the particle surface characteristics, the solid elasticity, and the particle loading. It is usually obtained from an experimental, effective thermal conductivity measurement under the required particle surface and loading conditions. In this study, an attempt is made to evaluate ϵ_A from the particle shape and properties.

Global-heat-transfer model

Radiant Heat-Transfer Coefficient. When the bed temperature is higher than 200°C, the radiation heat transfer between particles cannot be ignored. The radiation is a function of temperature, radiating surface, emissivity, and view factor. Following Wakao and Kato (1969), the radiant heat-transfer rate, Q_r, between the two hemispheres at temperature T_1 and T_2, is

$$Q_r = \frac{A\sigma}{2\left(\frac{1}{\omega} - 1\right) + \frac{1}{F_{12}}} (T_1^4 - T_2^4). \tag{7}$$

If a radiant heat-transfer coefficient h_r is used, the rate equation can be simplified, with

$$Q_r = Ah_r(T_1 - T_2) \tag{8}$$

$$h_r = \frac{\sigma}{2\left(\frac{1}{\omega} - 1\right) + \frac{1}{F_{12}}} (T_1 + T_2)(T_1^2 + T_2^2) \tag{9}$$

where ω is the emissivity of the gray surfaces, T_1 the particle temperature, and T_2 the average temperature of adjacent particles. The value $F_{12} = 0.576$ has been computed by Wakao and Kato (1969).

Quite often, the radiation heat transfer between the packed particles is expressed by a radiation thermal conductivity, k_r (Beveridge and Haughey, 1971; Harris and Lenz, 1985; Kung, 1972), as

$$q_r = -k_r \frac{\partial T}{\partial \xi} = h_r(T_1 - T_2). \tag{10}$$

Convection Heat-Transfer Coefficient. During tire pyrolysis, approximately 65% by weight of the rubber is decomposed and evaporated. The flow of volatile matter through the voids engenders a convection heat transfer between the fluid and the solid particles. The Reynolds number of the gas flow is expressed as

$$Re = \frac{d_p u_s \rho_g}{\mu} \tag{11}$$

where d_p is the particle diameter, u_s the superficial fluid velocity, ρ_g the fluid density, and μ the fluid viscosity.

Wakao and Kaguei (1984) reviewed the literature published on convection heat-transfer models at low and high Reynolds numbers. They proposed the following correlation to calculate the heat-transfer coefficient:

$$Nu = 2 + 1.1 Pr^{1/3} Re^{0.6} \tag{12}$$

where

$$Nu = \frac{h_c d_p}{k_g} \tag{13}$$

and

$$Pr = C_{Pg} \frac{\mu}{k_g}. \tag{14}$$

In these relations, h_c is the particle-to-fluid heat-transfer coefficient, d_p, the particle diameter, k_g, the fluid thermal conductivity, C_{Pg}, the specific heat of the fluid, and μ, the fluid viscosity.

The superficial fluid velocity can be determined by the global fluid velocity u and the global porosity ϵ, through the following relation:

$$u_s = \frac{u}{\epsilon} \tag{15}$$

where the value of u depends on the pressure gradient in the reactor.

Pressure Inside the Reactor. Uniform temperature and pressure are assumed in the upper gas space of the reactor, whose values are the mean values of the temperature and pressure in the mixed volatile materials from the bed of particles. The value of the mean pressure is related to the gas accumulation in the reactor, which is a dynamic process governed by the simultaneous ongoing volatilization process from the bed of particles and gas removal by the vacuum pump. The mass balance of volatile materials in the reactor over a small time step is given by

$$m_g = m_g^0 + \Delta m_b - \Delta m_p \tag{16}$$

where m_g^0 is the mass of volatiles at last time step; Δm_b is the mass increase due to the volatilization from the bed of particles, and Δm_p is the mass decrease induced by the vacuum pump. They are given by

$$\Delta m_b = \Sigma \Delta m_i \tag{17}$$

$$\Delta m_p = A \int \rho_g u \, dt \tag{18}$$

where ρ_g the velocity gas density, and u the velocity of gas flowing out of the reactor, are given by

$$u = \frac{Q_{\text{pump}}}{A} \tag{19}$$

where Q_{pump} is the volumetric velocity of the vacuum pump and V_g is the volume of the upper space of reactor. Finally the mean pressure is given by the ideal gas law equation

$$P_g V_g = m_g R T_g \tag{20}$$

where T_g is the mean temperature of the volatile gas.

Kinetics and heat of pyrolysis

Tires are made of a complex blend of elastomers, carbon black, processing oil, vulcanization agents and other additives. More than 90 wt. % of a tire is oil, elastomer, and carbon black. In North America, car tire treads and sidewalls are generally made of SBR, SBR/BR, NR/BR, NR/SBR, and NR/SBR/BR (Hofmann, 1989). Because the carbon black is inert during the pyrolysis process, the pyrolysis of oil and polymers governs the kinetics of tire pyrolysis.

Kinetics of Tire Pyrolysis. The pyrolysis kinetics of straight NR, SBR, and BR were investigated in previous studies (Sircar and Lamond, 1970, 1972, 1975; Yang et al., 1993). It was found that these elastomers pyrolyze when the temperature is in the range of 300–500°C. A first-order kinetic equation can be successfully used to represent the weight loss during the pyrolysis of the elastomers and the processing oil. This equation is written as

$$\frac{dm}{dt} = Ze^{-E/RT}(1 - m) \tag{21}$$

where m is the mass fraction of the mass of volatiles evaporated at time t, E is the apparent activation energy, and Z is the preexponential factor. These parameter values were determined in a previous study (Yang et al., 1993) and gave for oil $E = 49.1$ kJ/mol, $Z = 4.01 \times 10^4$ min^{-1}; for NR $E = 207$ kJ/mol, $Z = 2.36 \times 10^{16}$ min^{-1}; for SBR $E = 152$ kJ/mol, $Z = 1.78 \times 10^{10}$ min^{-1}; and for BR $E = 215$ kJ/mol, $Z = 6.32 \times 10^{14}$ min^{-1}.

The tire weight loss during pyrolysis can be viewed as a combined process of oil vaporization and volatilization of the pyrolyzed elastomers (Yang et al., 1993). A composite form of the first-order equation with Arrhenius parameters can then be used to describe the process (Flynn and Wall, 1966), which gives

$$\frac{dm}{dt} = \Sigma \alpha_i Z_i e^{-E/RT}(1 - m_i) \tag{22}$$

where α_i is the weight fractions, Z_i and E_i the preexponential factors and the apparent activation energies for oil and component elastomers, respectively. Figure 2 shows the rate of weight loss of the tire sidewall particles during the pyrolysis process as measured by TGA. The dashed line corresponds to the simulated curves using Eq. 22.

Enthalpy Change During Tire Pyrolysis. There are three parts of enthalpy change that should be considered during the tire pyrolysis: (1) sensible heat, for raising the temperature of a certain mass of material; (2) the heat of reaction, produced during the polymer thermal decomposition, which may be endothermic or exothermic; (3) the heat of volatilization, providing energy to evaporate the pyrolysis products. Figure 3 shows the overall enthalpy change measured by DTA and the contribution of sensible heat, the heat of reaction, and the heat of vaporization obtained by thermal analysis.

The sensible heat of tire was measured by DSC. Based on the measurement, a linear correlation of specific heat and temperature was obtained through the DSC curve simulations (Yang and Roy, 1994a):

$$C_p = 1.23 + 6.55 \times 10^{-3} T. \tag{23}$$

The heat of evaporation q_e is proportional to the rate of volatilization and is defined as

$$q_e = \Sigma h_{g_i} \frac{dm_i}{dt} \tag{24}$$

where i is the component materials and h_g is the latent heat of vaporization of the pyrolysis products and dm/dt the rate of weight loss that can be measured by thermogravimetry or calculated by Eq. 21. The m_i included both vapors and gases and in fact only the vapors will absorb heat to evaporate. Since the percentage of gases is usually low (ca. 5%), it will not introduce significant error in the calculation of q_e. The value of h_g was found to be 250 kJ/kg for NR and 280 kJ/kg for BR (Yang and Roy, 1995a).

The heat of reaction q_d is obtained by subtracting the sensible heat and the heat of evaporation from the total enthalpy change. It is assumed that the heat of reaction is proportional to the rate of decomposition of polymers, which yields

$$q_d = \Sigma h_{di} \frac{dC_i}{dt} \tag{25}$$

where h_d is the reaction heat coefficient and dC/dt is the rate of decomposition. The use of the first-order kinetic equation with Arrhenius parameters in Eq. 25 to model the rate of decomposition gives

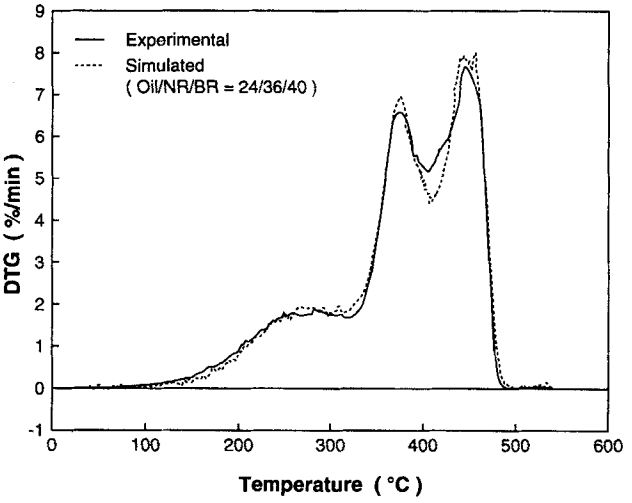

Figure 2. Tested and simulated DTG curves of used tire material (simulation based on 24% oil+36% NR+40% BR).

$$q_d = \Sigma h_{di} Z_i e^{-E/RT}(1 - C_i). \tag{26}$$

The values of h_d, E, and Z were determined in earlier studies (Yang et al., 1993), and are for NR $h_d = 214$ kJ/kg, $E = 207$ kJ/mol, $Z = 2.36 \times 10^{16}$ min^{-1}; for SBR $h_d = 500$ kJ/kg, $E = 207$ kJ/mol, $Z = 2.36 \times 10^{16}$; for BR $h_d = 760$ kJ/kg, $E = 207$ kJ/mol, $Z = 2.36 \times 10^{16}$.

Properties of packed bed

The packing of scrap tire particles is a random arrangement of granular and polydisperse tire particles, which are often heterogeneous in geometry, size, and the way the particles deposit. When tire particles are packed in the reactor, the arrangement of particles and the resulting void distribution between the particles may have a significant influence on

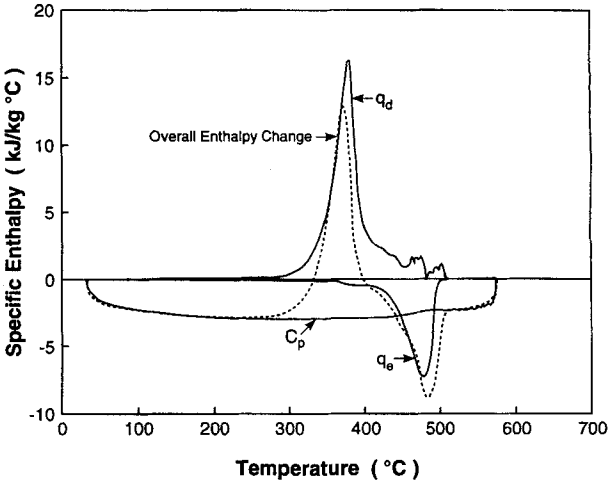

Figure 3. Overall enthalpy change and the contribution of the sensible heat C_p, the heat of reaction q_d, and the heat of evaporation q_e during tire pyrolysis.

the heat and mass transfer in the bed of particles. Several parameters are used to describe the packing properties.

In this work, the tire particles consisted of quasi-identical cylinders of diameter d_p and length L. A mean volume diameter (Vaněček et al., 1966) $\bar{d}$ was used to describe the grain size of particles:

$$\frac{\pi}{4}\overline{d^2}\,\overline{L} = \frac{\Sigma \frac{\pi}{4} d_p^2 L}{N}. \tag{27}$$

Since $\bar{d} = \bar{L}$ for the particles used in this experiment, the previous equation simplifies to

$$\bar{d} = \sqrt[3]{\frac{\Sigma d_p^3}{N}} \tag{28}$$

where N is the number of the particles in the bed. The pores in the packed bed are interconnected, which allows the volatile materials to flow between particles and finally move out of the bed. The porosity defined as the fraction of void to the bed total volume can be calculated by Eq. 29 (Scheidegger, 1960):

$$\epsilon = \frac{V_b - V_s}{V_b} \tag{29}$$

where V_b is the bed volume and V_s the volume of solid particles.

Mathematical Heat-Transfer Model

Five basic thermal and kinetic phenomena must be considered in this model: heat transfer from the reactor wall to the bed of particles; heat transfer from the outer surface to the core of the bed; the kinetics of tire pyrolysis reactions; the energy consumption or generation due to the endothermic or exothermic nature of the pyrolysis process; and the variation of the composition and the thermal properties of the tire particles. As these processes are thermally dependent, they are therefore a function of time during the heating process.

Previous studies revealed that when there are more than 10 particles in the radial direction and more than six in the axial direction, a pseudohomogeneous model can be used for the heat-transfer study, without causing significant errors (Hlavacek and Votruba, 1977). A pseudohomogeneous model considers the bed as continuous, where the separate phase contributions are averaged. A constant temperature at the bottom and lateral wall of the reactor, and thus a symmetry of revolution for the temperature field, are assumed (for instance, a molten lead bath reactor will fulfill those requirements). Therefore, a two-dimensional pseudo-homogeneous model is sufficient to represent the axial and radial heat-transfer phenomena.

Since the heat transfer in the reactor during pyrolysis is a complex phenomenon, some simplifications are necessary before a "workable" model can be developed:

1. The intraparticle convection is ignored. Conduction is the only heat-transfer phenomenon within the solid.
2. Conduction across the gas in the voids is ignored.
3. Radiation between particles exists only between adjacent particles.
4. The gas inside the reactor is transparent, so the absorption and reflection of the radiation by the gas are ignored.
5. The gas flow within the bed is only in the axial direction.
6. The pressure and temperature of the volatile materials are uniform everywhere in the reactor.

It is assumed that the domain of study consists of an array of small unit cells. As shown in Figure 1, every unit cell consists of solid particles and void space between particles. It is assumed that every cell has the same porosity, whose value is taken as the averaged bed porosity. Several heat-transfer mechanisms are considered for a unit cell: (1) conduction through the solid phase, the void space, and the contacting point of particles; the effective thermal conductivity k_e (Eq. 1) is used to calculate these three conductions; (2) radiation between particles, through the surface of every particle (the radiation heat exchange exists in both axial and radial direction), Eq. 10 is used to calculate the radiation thermal conductivity k_r; (3) convection heat transfer between particle surface and the flowing gas in the void space of cell. According to Eq. 12, the convection primarily depends on the flow rate and the thermal properties of the fluid. In this study, the fluid flow being mainly in the axial direction, the convection in the radial direction is omitted.

For the thermal modeling of the pyrolysis process, one should consider the two temperature windows that correspond to the nonreactive zone ($T < 200$°C) and the reaction zone ($T \geq 200$°C). From a practical standpoint, just one set of equations is used to describe the heat-transfer phenomena in the two zones. The equations will automatically fit the case with $h_c \approx 0$ and $k_r \ll k_e$, when $T < 200$°C.

Considering the enthalpy change of a unit cell, the conduction and radiation between particles, the convection between particle and gas, and the heat generation or consumption of pyrolysis, the energy balance of a unit cell can be expressed as follows:

$$[\epsilon_{\rho_p} C_{Pg} + (1-\epsilon)\rho_s C_{Ps}]\frac{\partial T}{\partial t} = \frac{1}{r}\frac{\partial}{\partial r}\left(rk_e\frac{\partial T}{\partial r}\right) + \frac{\partial}{\partial z}\left(k_e\frac{\partial T}{\partial z}\right) + \frac{1}{r}\frac{\partial}{\partial r}\left(rk_r\frac{\partial T}{\partial r}\right) + \frac{\partial}{\partial z}\left(k_r\frac{\partial T}{\partial z}\right) + \beta h_c\left(\frac{\partial T}{\partial z}\right) + (1-\epsilon)\rho_s q \tag{30}$$

where $\epsilon\rho_g C_{Pg}(\partial T/\partial t)$ and $(1-\epsilon)\rho_s C_{Ps}(\partial T/\partial t)$ are the enthalpy changes for the gas and the solid, respectively; the conduction between particles is given by $1/r\partial/\partial r(rk_e\partial T/\partial r) + \partial/\partial z(k_e\partial T/\partial z)$. The radiation between cells is represented by $\partial/\partial r(rk_r\partial T/\partial r)/r + \partial/\partial z(k_r\partial T/\partial z)$; the convection is only in the axial direction, and is given by $\beta h_c(\partial T/\partial t)$, where β is the area factor defined as the ratio of the surface area of particles in one cell to the surface area of unit cell; the heat source due to the pyrolysis reaction is given by $(1-\epsilon)\rho_s q$,

which consists of the heat of evaporation q_e (Eq. 24) and the heat of reaction q_d (Eq. 26).

The term ρ_b is defined as the bed density, which can be represented as $(1-\epsilon)\rho_s$. Since the bed pressure is very low, $\rho_g C_{Pg} \ll \rho_s C_{Ps}$. Then Eq. 30 simplifies to

$$\rho_b C_{Ps} \frac{\partial T}{\partial t} = \frac{1}{r}\frac{\partial}{\partial r}\left[r(k_e + k_r)\frac{\partial T}{\partial r}\right] + \frac{\partial}{\partial z}\left[(k_e + k_r)\frac{\partial T}{\partial z}\right] + \beta h_c\left(\frac{\partial T}{\partial z}\right) + \rho_b q. \quad (31)$$

Heat transfer from the reactor to the bed

The energy source for the heating process is the high-temperature reactor wall. The heat is transferred from the reactor to the bed through the boundary surfaces. Figure 4 indicates the boundary conditions of a packed bed during a heating process. At $z = 0$, particles are in close contact with the bottom wall, thus $T = T_w$. At the top surface ($z = L$), particles are exposed to the radiation flux from the upper space of the reactor (ω is the emissivity of particle and F the view factor). At the lateral surface, radiation dominates; the view factor is considered as 1, due to the small distance between the bed and the reactor wall.

Numerical solution

Since the energy balance equation (Eq. 31) is highly nonlinear, it cannot be solved analytically. In the present study, a finite difference method is used to approximate the heat-transfer equation. The computational domain is $0 \le z \le L$, $0 \le r \le R$ and $t \ge 0$. A regular mesh was used on the domain, which comprises $(n+1)\times(m+1)$ points on each time line, with $n\Delta z = L$ and $m\Delta r = R$. The time increment is Δt. In calculations, the values of m and n are taken as 30, and $\Delta t = 10$ seconds. A mesh analysis was carried out and no mesh effects were found.

The governing equation expressed in a finite difference form is as follows:

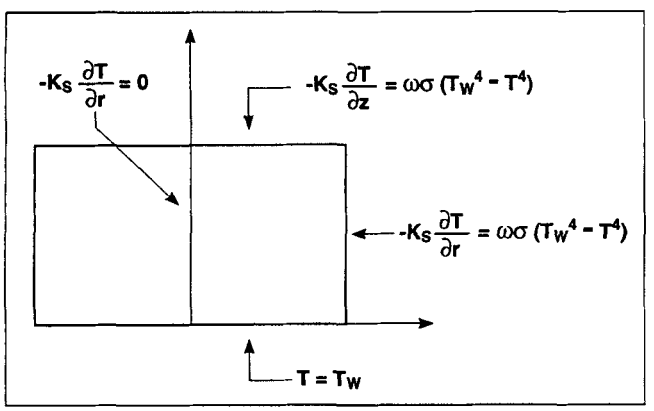

Figure 4. Boundary conditions of the packed bed of tire particles during the heating process.

$$\frac{\rho_{i,j} C_{P_{i,j}}}{\Delta t}\left(T_{i,j} - T_{i,j}^{n-1}\right) = \frac{r_{i+1/2}}{r_i \Delta r^2}(k_e + k_r)_{i+1/2,j}(T_{i+1,j} - T_{i,j}) - \frac{r_{i-1/2}}{r_i \Delta r^2}(k_e + k_r)_{i-1/2,j}(T_{i,j} - T_{i-1,j}) + \frac{1}{\Delta z^2}(k_e + k_r)_{i,j+1/2}(T_{i,j+1} - T_{i,j}) - \frac{1}{\Delta z^2}(k_e + k_r)_{i,j-1/2}(T_{i,j} - T_{i,j-1}) + \frac{\beta h_c}{\Delta z}(T_g - T_{i,j}) + \rho_{i,j} q_{i,j} \quad (32)$$

where i (respectively, j) denotes the grid locations on the r axis (respectively, z axis) and where n represents the time index.

The resolution of this equation is based on the alternating direction implicit (ADI) method (Jaluria and Torrance, 1986). The ADI method uses an explicit formulation in one direction and an implicit formulation in the other. The directions are alternated from one iteration to the next. The flow chart of the computer program is shown in Figure 5. The program was written in Fortran 77 and simulations were run on a VAX/VMS minicomputer.

To run the simulations, the following input data must be provided: (1) wall temperature of the batch reactor; (2) thermal properties of tire particles; (3) kinetic properties of tire pyrolysis; and (4) properties of the packed bed.

Model Predictions and Discussion

Predictions of the transient temperature and density distributions in the tire-bed, and the overall mass change, energy consumption are given in this section. The predictions are based on the assumptions that the reactor wall temperature is constant at 510°C during the whole pyrolysis process. The initial load of scrap tires is 3.4 kg. Tables 1 to 3 illustrate the values for the different properties used in the computations. It was found that the model was not very sensitive to the input parameters.

Temperature history and energy change

Figure 6 shows the predicted time evolution of the temperature at the center of the bed at various heights during tire pyrolysis. At time $t > 0$, an intensive heat transfer from the reactor to the bed appears on the boundary surfaces, due to the large temperature difference between the reactor and the bed. In Figure 6, a rapid temperature increase is observed at the bottom and top surfaces of the bed. At $z = 0$ (the bottom surface of the bed), the particle temperature jumps from room temperature to 510°C, due to the direct contact with the reactor. At $z = 1$ (the top surface of the bed), a rapid temperature increase is also observed due to the intensive radiant heat projected on the surface.

The typical shape of the temperature curves at the onset of the heating process can be explained by the large thermal resistance that exists between the boundary surfaces and the center of the bed. During the first 20 minutes, the heat flux to the bed is high, which results in noticeable temperature

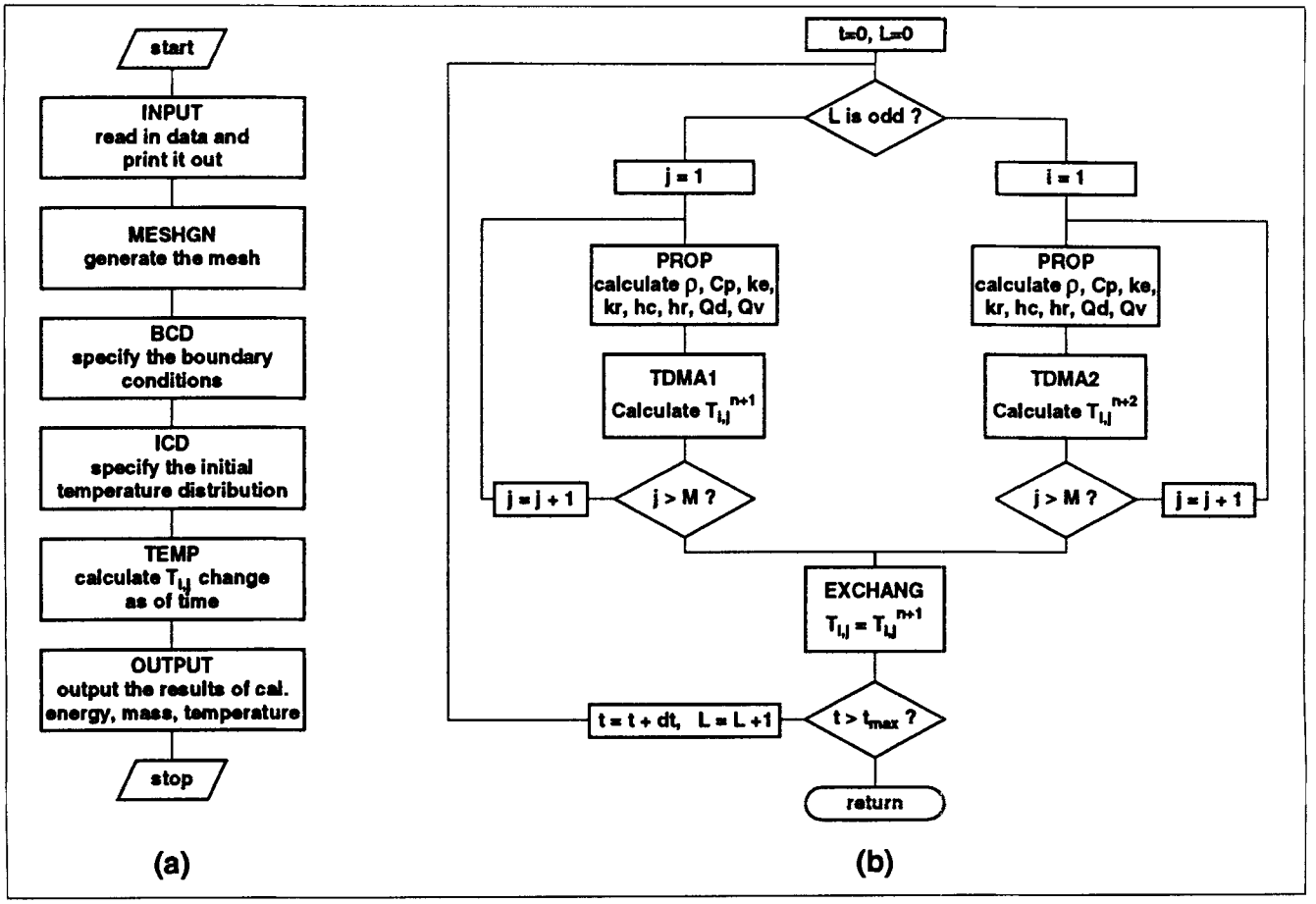

Figure 5. Flow chart of the computer program.

(a) Flow chart of the main program. (b) flow chart of the subroutine TEMP.

gradients. Later, when the bed temperature becomes higher, the heat flux to the bed tends to decrease which, in turn, lowers the temperature gradients. This phenomenon is undoubtedly caused by an increase of the effective thermal conductivity with the temperature rise, which causes smaller temperature gradients in the bed. At a later stage of the heating process, the interparticle radiations increase significantly with the increase in the bed temperature and become the dominant heat-transfer mechanism. (The radiation is about twice as high as the thermal conduction when temperature rises to 500°C.)

Table 1. Reactor and Packed-Bed Conditions and Characteristics

Initial temperature of the bed	$T_0 = 25$°C
Initial pressure of the bed	$P_0 = 0$ kPa
Temperature of the reactor wall	$T_w = 510$°C
Radius of the reactor	$R_{max} = 0.1$ m
Height of the reactor	$H = 0.2$ m
Packed-bed porosity	$\epsilon = 0.4$
Mean diameter of the cylindrical tire particles	$d_p = 0.005$ m

The temperature history in Figure 6 reflects both the thermal and kinetic changes in the bed. Before 300°C the temperature increase is roughly linear, while there is no significant chemical reactions involved. While the temperature further increases, upward and downward peaks appear, showing the beginning of the reactions of tire pyrolysis. In the temperature range 300–450°C, the elastomers in the tires decompose, and heat is released. In the temperature range 200–500°C, the pyrolysis products and other low-boiling-point materials are evaporated, which results in endothermic en-

Table 2. Thermal Properties

Variable	Value	Unit	Reference
True density of tire, ρ	1,150	kg/m^3	Present work
Specific heat of tire (at 0°C), C_p	1,230	J/kg·K	Yang and Roy (1995a)
Thermal conductivity of tire, k	0.3	W/m·K	Sircar et al. (1988)
Specific heat of carbon black, C_{pcb}	850	J/kg·K	Touloukian (1970)
Viscosity of volatile material, μ	10	mm^2/s	Schuman et al. (1978)

Table 3. Kinetic Properties*

Properties	Oil	NR	BR	Carbon Black
Fraction α_i	0.17	0.25	0.28	0.3
Preexperimental factor Z (1/min)	4.01×10^4	2.36×10^{16}	6.32×10^{14}	—
Activation energy E (kJ/mol)	49.1	207	215	—
Heat of reaction (kJ/kg)	—	215	760	—
Heat of vaporization (kJ/kg)	250	280	280	—

*All data from Yang et al. (1993; 1995a).

ergy changes. At this point, the sample compositions, density, and specific heat are modified. Finally, at $t = 100$ min, when the average bed temperature rises to 500°C and the extent of conversion of the tire bed reaches 99%, the pyrolysis process is considered to be complete.

The temperature distribution in Figure 6 is not symmetric around the axial axis. The lowest temperature is found at the position of $z = 0.6$. This can be explained by the fact that a larger portion of the thermal energy is transferred through the bottom than through the top surface.

Figure 7 exhibits the heat transfer from the reactor wall to the bed of tire particles. The heat transfer through the bottom of the reactor where both conduction and radiation exist due to the contact of tire particles and reactor is Q_1; Q_2 is the heat transfer through the lateral and top surfaces of bed induced by radiation. It can be observed in Figure 7 that 35% of the heat transfer to the bed is through the bottom surface, 25% through the top surface, and 40% through the lateral surface. The most efficient heating occurs during the first 20 minutes, during which about 50% of the total energy is transferred from the reactor to the bed.

In Figure 7 Q_{tot} represents the total heat transfer to the bed through the boundaries. At the end of the pyrolysis, Q_{tot} is calculated as 3,077 kJ. Since the mass of feedstock is equal to 3.4 kg, the total energy consumption per kilogram of tire is 905 kJ/kg. This result is close to the value of 706 kJ/kg estimated experimentally by Labrecque (1987).

As a result of the heat being transferred to the bed, the bed energy increases with time (Figure 8), which is used to warm up the unreacted zone and drive the pyrolysis reaction. In Figure 8, Q_s is the sensible heat, Q_p the heat of decomposition, and Q_e the heat of evaporation. Before pyrolysis, about 670 kJ/kg of energy is needed to heat the particles from room temperature to the more intense pyrolysis temperature level, that is, about 300°C. When tire pyrolysis proceeds, approximately 200 kJ of energy is released by each kilogram of elastomers decomposing, which provides an extra heat source to the bed. The vaporization of the pyrolysis products is endothermic; about 180 kJ/kg of energy is consumed during the vaporization process. The energy calculation indicates that the major portion of the energy consumption in tire pyrolysis goes into the increase of the sample internal energy. The evaporation heat takes about 20% of the total energy consumption. The decomposition heat provides about 22% extra heating. Any analysis ignoring the heat of reactions would discard important thermal mechanisms.

Density change

Figure 9 exhibits the density history in the center of the bed, corresponding to the temperature changes shown in Figure 6. In Figure 9, three regions can be observed from every density curve, namely the virgin, the reactive, and the carbon black regions. The virgin region (before pyrolysis occurs) is characterized by a constant sample density of 763 kg/m^3. For the second region, tire pyrolysis occurs that results in dramatic density changes. During pyrolysis, the sample volumet-

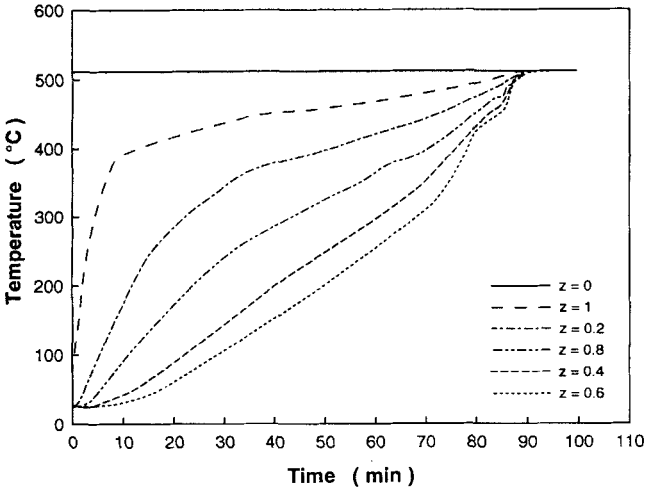

Figure 6. Temperature history at the center of bed and various heights during tire pyrolysis.

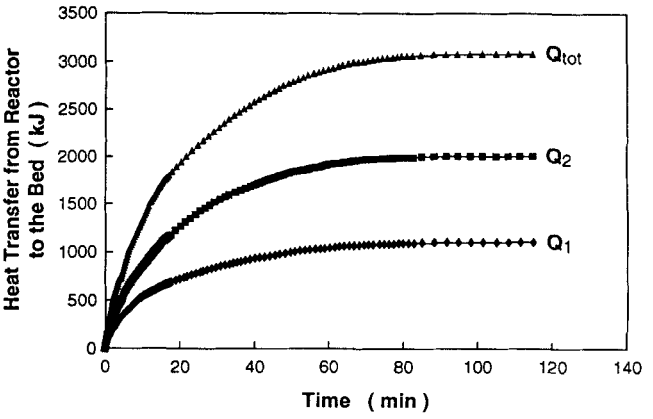

Figure 7. Heat transfer from the reactor to the bed.

Q_1—Heat transfer through the bottom surface; Q_2—heat transfer through the top and lateral surfaces of bed; Q_{tot}—the total heat transfer to the bed through the boundary surfaces.

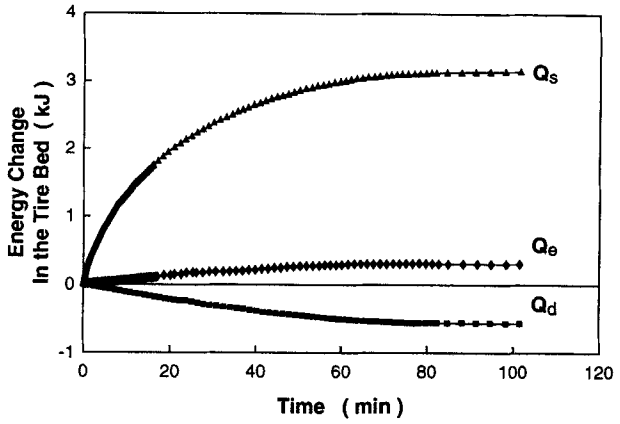

Figure 8. Sensible heat Q_s, evaporation heat Q_e, and heat of reaction Q_d during pyrolysis of the bed of tire particles.

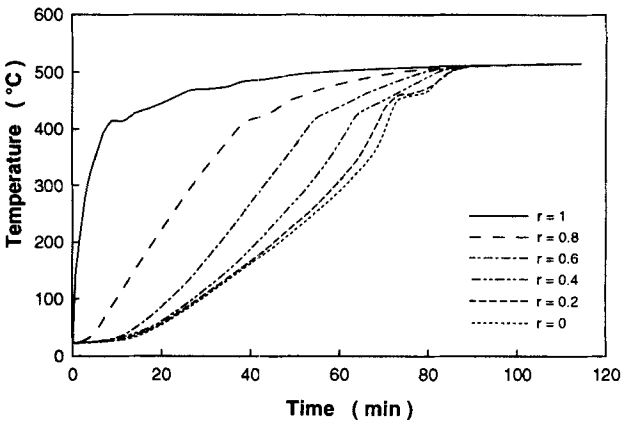

Figure 10. Temperature history in the radial direction at an axial position of $z = 0.6$.

ric shrinkage or expansion is small, and the pyrolysis products are assumed to leave the matrix of particles as soon as they are formed. The local density change is therefore determined by the sample's weight loss process caused by the vaporization of pyrolysis products. In the reaction region, three steps of weight loss can be observed from the density curves. It is caused by the different pyrolysis temperatures of oil, NR and BR. The third region is when pyrolysis is completed and the sample density becomes constant again. The sample final density is 250 kg/m^3, corresponding to the 70 wt. % loss during tire pyrolysis. The residual material is carbon black, which proximate analysis says is 80% fixed carbon (Labrecque, 1987). Since the volume change is minor during pyrolysis, the carbon-black residue has a microporous structure.

Heat-transfer and pyrolysis mechanism in the bed

Figures 10 and 11 illustrate the temperature and density changes with the radial direction at an axial position $z = 0.6$. The physical phenomena represented are the heat and reaction front propagation, from the border toward the center of the bed. Heat is transferred mainly by conduction and radiation. When $T < 200$°C, the contribution of radiation is around five times less than that of conduction. When $T > 200$°C, the contribution of radiation quickly increases, and eventually becomes the major mechanism for intraparticle heat transfer. Convection is also present, which is produced by the flow of volatile materials in the void spaces. The computations, however, show that the convection for the existing low-pressure conditions is several orders of magnitude less than the conduction or the radiation.

The pyrolysis process presented in Figure 10 can be regarded as a reactive front advancing into the virgin tire, leaving behind it a thoroughly converted material. The advancing rate of the front determines the rate of pyrolysis propagation. Pyrolysis occurs over a temperature range of 200–500°C. At the reactive front, a jump of temperature and density occurs when there is a sudden weight loss and a drop in the value of C_p caused by the tire pyrolysis reaction.

Depending on the characteristic times of heat transfer and the extent of pyrolysis, the tire pyrolysis can be either con-

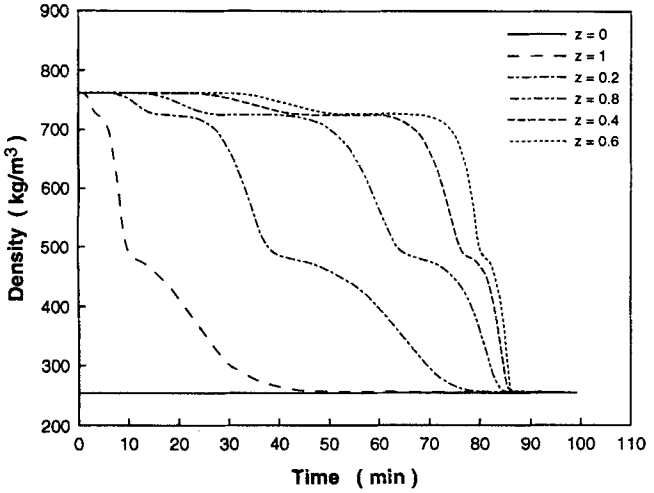

Figure 9. Density variation at the center of the bed and various heights during tire pyrolysis.

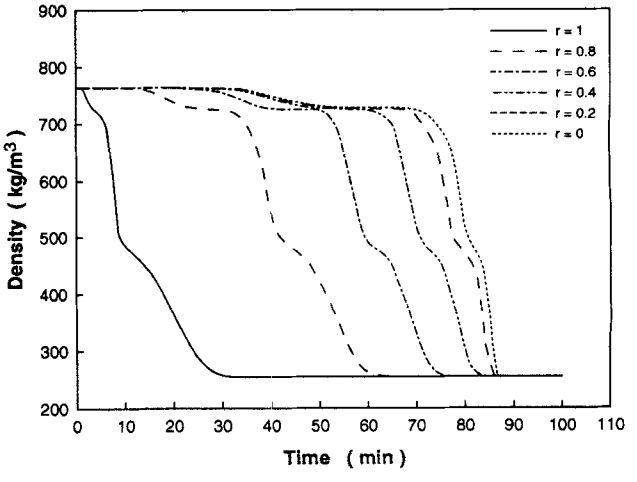

Figure 11. Density variation in the radial direction at an axial position of $z = 0.6$.

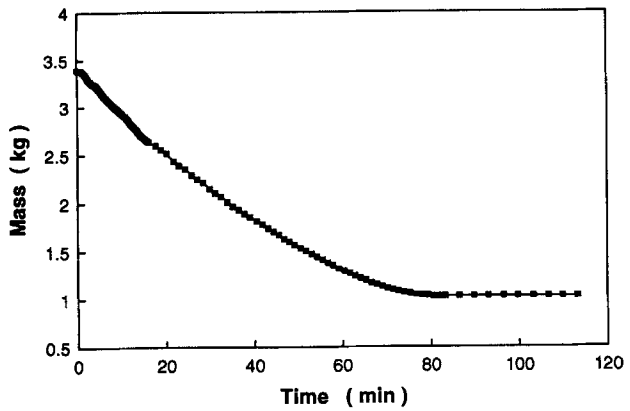

Figure 12. Overall mass loss of the tire bed as a function of time.

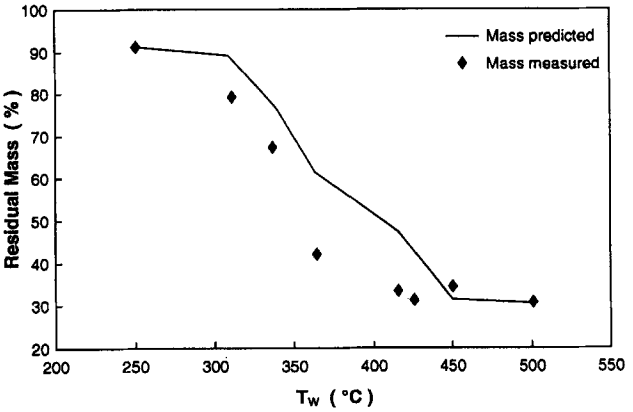

Figure 13. Residual yield as a function of reactor wall temperature T_w.

trolled by the heat transfer or by the kinetics. The characteristic time for the heat transfer in the bed can be estimated by $\tau_t = C_p R^2/K$, where R is the radius, ρ the density, C_p the specific heat, and K the overall effective thermal conductivity, and for the pyrolysis by $\tau_r = 1/k$, where $k = Z \exp(-E/RT)$. In our case, τ_t was about 10^5 s, and τ_r was 10^2 s, which shows that the process is heat-transfer controlled.

Mass loss history

Figure 12 shows the overall mass loss of the bed as a function of time. The initial bed weight is 3.4 kg. After pyrolysis, the bed weight becomes 1.02 kg, that is, 30% of its initial weight. Unlike the weight loss behavior of a single particle, which is basically kinetic controlled (see Figure 3), the weight loss history of the bed of tires is determined by both the heat transfer and kinetic processes of tire pyrolysis, and a gradual weight loss process can be observed in Figure 12.

The relationship between the reactor temperature T_w and the residual yield, which reflects the extent of pyrolysis, has an important practical interest. Experimental measurements can be found elsewhere (Bouvier et al., 1987; Labrecque, 1987; William et al., 1990). In the present article, the residual yield is directly predicted by the computations. Figure 13 shows the predicted variation of the residual yield with the reactor temperature, which in turn was compared with the experimental measurements made by Labrecque. The overall trend of the prediction is fair, although discrepancies are observed for several of the discrete data points.

To better illustrate the residual yield change with T_w, the energy provided by the reactor to the tire bed was calculated. When $T_w = 250$°C, the heat provided to the bed is 497 kJ/kg. This amount of energy is not high enough to initiate the tire pyrolysis reactions; 96% of the initial weight is thus left as a residual yield. The 4% weight loss is attributed to the vaporization of some low-boiling-point materials in the tire particles. When $T_w = 415$°C, the heat provided to the bed reaches 786 kJ/kg and the yield of solid residue predicted is 47% (Figure 13). At this temperature, tire pyrolysis is occurring but there is not enough energy for the reaction to be completed. Previous studies have shown that tire pyrolysis products have complex composition. Their evaporation requires that energy is provided on a continuous basis over a large temperature band. According to the model, if $T_w < 450$°C, the energy transferred to the bed will not be enough to complete the evaporation process. Consequently, some pyrolysis products will remain in the bed, resulting in high yield of solid residues as shown in Figure 13.

Comparison between the measured and the predicted bed temperature

To validate the model, a comparison between the measured and predicted temperature history in the tire bed was made and is illustrated in Figure 14.

The tire pyrolysis experiment was previously performed by Labrecque (1987) in an electrically heated reactor. The electric heating system provided a gradual temperature increase in the reactor wall. A thermocouple was fixed in the center of the bed. A vacuum pump with a volumetric flow-rate capacity of 0.5 m^3/min was connected with the reactor to maintain the low pressure in the reactor. The initial mass of the tire bed was 1 kg. The scrap-tire particles were cylindrical, with a diameter varying between 5 and 12 mm. The particles were taken from cross-ply tire sidewalls. Their average composition was determined to be oil:NR:BR:carbon black =

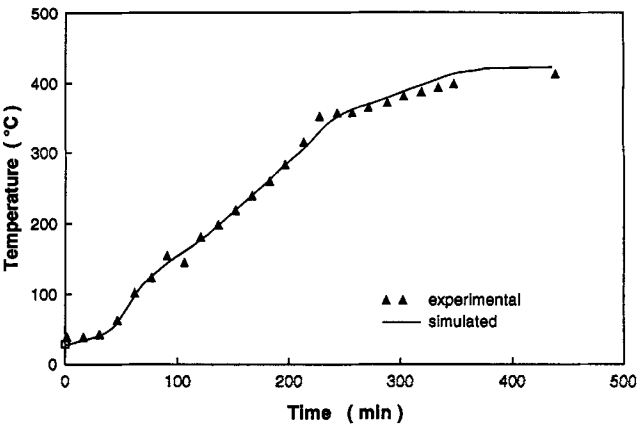

Figure 14. Measured and predicted temperature history at the center of bed.

17:25:28:30, based on the thermogravimetry analysis of a tire sidewall sample, as shown in Figure 2.

In Figure 14, an excellent agreement can be found between these two results before the pyrolysis proceeds after about 200 min. After 200 min, the agreement is still fairly good, although the predicted exothermic peak occurs about 30 min later than in the experiment. Also, the predicted temperature is slightly above the experimental temperature once the pyrolysis is complete.

Pressure evolution

The pressure inside the reactor is a very important factor during vacuum pyrolysis reactions. Previous studies have shown that the quantity and quality of pyrolysis oils and carbon black are strongly influenced by the pyrolysis pressure (Labrecque, 1987). A low pressure in the reactor promotes a fast elimination of the pyrolysis products from the particles, and thus minimizes possible secondary reactions such as thermal cracking and repolymerization.

The gas density in the reactor is governed by the mass balance between the gas production and the gas flow out of the reactor. For the overall process, the pressure history is related to the rate of pyrolysis reaction and the capacity of the vacuum pump.

Figure 15 shows the pressure changes in the pyrolysis process, as predicted by the model and measured by the experiment (Labrecque, 1987). A qualitatively good agreement is obtained. A similar shape is observed for the two pressure curves, including a major peak at 220–240 min, a small peak at 290–320 min, and two other minor peaks at 45 and 120 min, respectively. The major peak is believed to originate from the pyrolysis of tire that releases a large amount of volatile materials, resulting in an increase in pressure. The small peak may come from a different rubber material that has a higher stability. Let's recall that, in this simulation, the composition of tire sidewall was assumed as oil/NR/BR/carbon black = 17/25/28/30 and was based on a thermogravimetric analysis. On the other hand, tires used in Labrecque's work were collected from waste sidewall tires, possibly with different trademarks, which may exhibit some differences in composition. As for the two minor pressure peaks (just before the major one), these differences originate from the evaporation of low-molecular-weight additives such as processing oil.

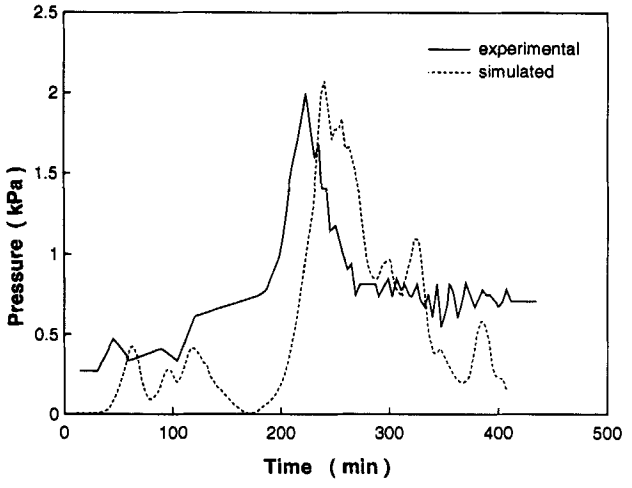

Figure 15. Pressure history in the pyrolysis reactor.

It can be noted that there is a shift of about 20 to 30 min toward the higher temperature between the numerical and experimental results. Although the reason for this shift is still unclear, the difference in chemical composition and component ratio between the experimental and theoretical systems can be part of the explanation. The higher base pressure of about 0.25 kPa in the experimental result is not surprising, because of unavoidable air leakage in the vacuum system.

Conclusion

A novel transient two-dimensional mathematical model of the thermal and kinetic processes during tire pyrolysis in a batch scale reactor was developed and tested.

This model is based on the microscopic studies of the pyrolysis of a small unit cell in a bed of the tire particles, and includes the following mechanisms: intra- and interparticle heat transfers; tire enthalpy changes; pyrolysis reactions; and thermal property changes during pyrolysis. The macroscopic properties of the tire bed are modeled by considering the pyrolysis behavior of all the unit cells. Theories previously developed from both microscopic and macroscopic studies of tire pyrolysis are incorporated in this model, including the studies of thermal and kinetic behavior of tire pyrolysis in tiny particles; the heat and mass transfer during the pyrolysis of a single particle; and the heat and mass transfer in a packed bed of particles.

The computational results of this model provide more precise and detailed data than those found in previous tire pyrolysis studies, leading to an improved understanding of the pyrolysis mechanisms for a bed of tire particles. These data include the thermal and kinetic properties of every unit cell, the rate of heat and pyrolysis propagation in the bed, and the overall mass, energy, and pressure changes in the reactor. Satisfactory accuracy of the computational results has been demonstrated through a comparison with the experimental data of Labrecque (1987).

Although this model was developed for a batch scale vacuum pyrolysis reactor, its fundamental equations, based on the microscopic description of tire pyrolysis mechanisms, should be directly applicable for the modeling of larger scale used tire batch pyrolysis reactors.

Notation

A = area, m^2
C_{P_s} = specific heat of the solid phase, $J \cdot kg^{-1} \cdot K^{-1}$
h_c = convection heat-transfer coefficient, $W \cdot m^{-2} \cdot K^{-1}$
m_g = mass of gases and vapors in the reactor, kg
n = time index
Nu = Nusselt number
P_g = mean pressure of gases and vapors in the reactor, $N \cdot m^{-2}$
Pr = Prandtl number
q_r = radiation heat flux, $W \cdot m^{-2}$
r = radial coordinate, m
R = ideal gas constant, $J \cdot K^{-1} \cdot mol^{-1}$
X = thermal conductivity ratio (k_s/k_g)
Y = effective thermal conductivity ratio (k_e/k_g)
z = axial coordinate, m

Greek letters

α = ratio factor
α^* = equivalent to $\alpha\epsilon_{A2}$
β = area factor
ρ_s = density of the solid, $kg \cdot m^{-3}$
σ = Stefan-Boltzmann constant, 5.67×10^8 $W \cdot m^{-2} \cdot K^{-4}$
ξ = space length in the direction normal to the particle surface, m

Literature Cited

Alula, M., D. Cagniant, and J. C. Lauer, "Contribution to the Characterization of Pyrolysis Coal Products by Means of Thermal Analysis," *Fuel*, **69**, 177 (1990).

Araki, T., K. Niikawa, H. Sosoda, H. Nishizaki, and S. Mitsui, "Development of Fluidized-Bed Pyrolysis of Waste Tires," *Conserv. Recycl.*, **3**, 155 (1979).

Argo, W. B., and J. M. Smith, "Heat Transfer in Packed Bed," *Chem. Eng. Prog.*, **49**, 443 (1953).

Bamford, C. H., J. Crank, and D. H. Malan, "The Combustion of Wood," *Proc. Cambridge Phil. Soc.*, **42**, 166 (1946).

Becker, H. A., A. M. Phillips, and J. Keller, "Pyrolysis of White Pine," *Combust. Flame*, **58**, 163 (1984).

Beveridge, G. S. G., and D. P. Haughey, "Axial Heat Transfer in Packed Bed-Stagnant Beds between 20 and 750°C, *Int. J. Heat Transf.*, **14**, 1093 (1971).

Bouvier, J. M., F. Charbel, and M. Gelus, "Gas Solid Pyrolysis of Tire Wastes Kinetics and Material Balances of Batch Pyrolysis of Used Tires," *Resour. Conserv.*, **1**, 205 (1987).

Brazier, D. W., and G. H. Nickel, "Thermoanalytical Methods in Vulcanizate Analysis II. Derivative Thermogravimetric Analysis," *Rubber Chem. Technol.*, **48**, 661 (1975).

Brazier, D. W., and N. V. Schwartz, "The Effect of Heating Rate on the Thermal Degradation of Polybutadiene," *J. Appl. Poly. Sci.*, **22**, 113 (1978).

Chambers, C., J. W. Larsen, W. Li, and B. Wleesen, "Polymer Waste Reclamation by Pyrolysis in Molten Salts," *Ind. Eng. Chem. Process Des. Dev.*, **23**, 648 (1984).

Chan, W. R., M. Kelbon, and B. B. Krieger, "Modelling and Experimental Verification of Physical and Chemical Processes during Pyrolysis of a Large Biomass Particle," *Fuel*, **64**, 1505 (1985).

Che, S. C., W. D. Deslate, and K. Duraiswamy, "The Occidental 'Flash Pyrolysis' Process for Recovering Carbon Black and Oil from Scrap Rubber Tires," Intersociety Conf. on Environmental Systems, San Diego, CA (July 12–15, 1976).

Flynn, J. H., and L. A. Wall, "General Treatment of the Thermogravimetry of the Polymers," *J. Res. Nat. Bur. Stand. 70A*, **6**, 487 (1966).

Harris, J. A., and T. G. Lenz, "Experimental Heat Transfer in a Packed Bed in which Radiation, Conduction and Convection are all Significant," *Proc. Nat. Heat Transf. Conf.*, Denver (Aug., 1985).

Havens, J. A., J. R. Welker, and C. M. Sliepcevich, "Pyrolysis of Wood: A Thermoanalytical Study," *J. Fire Flammability*, **2**, 321 (1971).

Hlavacek, V., and J. Votruba, "Steady-state Operation of Fixed-bed Reactors and Monolithic Structures," *Chem. Reactor Theory, A Review*, L. Lapidus and N. R. Amundson, eds., Prentice-Hall, New York (1977).

Hofmann, W., *Rubber Technology Handbook*, Oxford University Press, New York (1989).

Jaluria, Y., and K. E. Torrance, *Computational Heat Transfer*, Hemisphere, New York (1986).

Kung, H. C., "A Mathematical Model of Wood Pyrolysis," *Combust. Flame*, **18**, 185 (1972).

Labrecque, B., "Etude du Transfert de Chaleur par Radiation Thermique dans un Réacteur de Pyrolyse sous Vide des Vieux Pneumatiques," *Mémoire de Maîtrise*, Univ. Laval, Québec (1987).

Mahajam, O. P., A. Tomita, and P. L. Walker, "Differential Scanning Calorimetry Studies on Coal: 1. Pyrolysis in an Inert Atmosphere," *Fuel*, **55**, 63 (1976).

Maurer, J. J., "Advances in Thermogravimetric Analyses of Elastomer Systems," *J. Macromol. Sci. Chem.*, **A8**(1), 73 (1974).

Maurer, J. J., "Elastomer," in *Thermal Characterization of Polymer Material*, Chap. 6, E. T. Turi, ed., Academic Press, New York, p. 571 (1981).

Muñoz-Guillena, M. J., A. Linares-Solana, and C. Salinas-Martinez de Lecea, "Determination of Calorific Values of Coals by Differential Thermal Analysis," *Fuel*, **71**, 579 (1992).

Phuoc, T. X., and P. Durbetaki, "Heat and Mass Transfer Analysis of a Coal Particle Undergoing Pyrolysis," *Int. Heat Mass Transf.*, **30**(11), 2331 (1987).

Pyle, D. L., and C. A. Zaror, "Heat Transfer and Kinetics in the Low Temperature Pyrolysis of Solids," *Chem. Eng. Sci.*, **39**(1), 147 (1984).

Roy, C., B. de Caumia, J. Yang, and P. Plante, "Evaluation of the Vacuum Pyrolysis Process," Bioenergy R and D Seminar, Ottawa, Ont., Canada, p. 24 (Apr., 1989).

Roy, C., B. Labrecque, and B. de Caumia, "Recycling of Scrap Tires to Oil and Carbon Black by Vacuum Pyrolysis," *Resour., Conserv. Recycl.*, **4**, 203 (1990).

Scheidegger, A. E., *The Physics of Flow through Porous Media*, Univ. of Toronto Press, Toronto (1960).

Schulman, B. L., and P. A. White, "Pyrolysis of Scrap Tires Using the Tosco II Process," Reprint, Amer. Chem. Soc. Symp. Solid Waste and Residue (1978).

Sircar, A. K., and T. G. Lamond, "Determination of Butadiene in SBR-Type Copolymers by Thermographic Analysis," *J. Appl. Poly. Sci.*, **17**, 1327 (1970).

Sircar, A. K., and T. G. Lamond, "Identification of Elastomers by Thermal Analysis," *Rubber Chem. Technol.*, **45**, 329 (1972).

Sircar, A. K., and T. G. Lamond, "Identification of Elastomers in Tire Section by Total Thermal Analysis: I. Tread and Black Sidewall," *Rubber Chem. Technol.*, **48**, 301 (1975).

Sircar, A. K., and J. L. Wells, "Thermal Conductivity of Elastomer Vulcanizates by Differential Scanning Calorimetry," *Rubber Chem. Tech.*, **55**, 141 (1988).

Stevenson, A. J., G. R. Thomas, and D. G. Evans, "Modelling the Ignition of Brown-coal Particles," *Fuel*, **52**, 281 (1973).

Touloukian, Y. S., and E. H. Buyco, *Thermophysical Properties of Matter*, Vol. 5, IFI/Plenum Data Corp., New York, 1650 pp. (1970).

Vaněček, V., M. Markvart, and R. Drbohlav, *Fluidized Bed Drying*, Hill, London (1966).

Wakao, N., and K. Kato, "Effective Thermal Conductivity of Packed Beds," *J. Chem. Eng. Japan*, **2**, 24 (1969).

Wakao, N., S. Kaguei, and T. Funazkri, "Effect of Fluid Dispersion Coefficients on Particle-to-Fluid Heat Transfer Coefficients in Packed Beds. Correlation of Nusselt Numbers," *Chem. Eng. Sci.*, **34**, 325 (1979).

Wakao, N., and S. Kaguei, *Heat and Mass Transfer in Packed Beds*, Gordon and Breach, New York (1984).

Willliam, P. T., S. Besler, and D. T. Taylor, "The Pyrolysis of Scrap Automotive Tyres," *Fuel*, **69**, 1505 (1990).

Yagi, S., and D. Kunii, "Studies on Effective Thermal Conductivities in Packed Bed," *AIChE J.*, **13**, 373 (1957).

Yang, J., S. Kaliaguine, and C. Roy, "Improved Quantitative Determination of Elastomers in Tire Rubber by Kinetic Simulation of DTG Curves," *Rubber Chem. Technol.*, **66**, 213 (1993).

Yang, J., and C. Roy, "Study of the Energy Change during Tire Pyrolysis," in preparation (1995a).

Yang, J., P. A. Tanguy, and C. Roy, "A Combined Thermal and Kinetic Model for the Pyrolysis in a Single Tire Particle," *Chem. Eng. Sci.*, accepted (1995b).

Zaror, C. A., and D. L. Pyle, "The Pyrolysis of Biomass: A General Review," *Proc. Indian Acad. Sci. (Eng. Sci.)*, **5**, 269 (1982).

Manuscript received Jan. 21, 1994, and revision received Aug. 8, 1994.